Nonlinear ambipolar drift and periodic structure of a low-temperature, high-pressure plasma

A. V. Dem'yanov, D. A. Mazalov, A. P. Napartovich, A. F. Pal', and V. V. Pichugin

Troitsk Institute of Innovative and Thermonuclear Research, 142092 Troitsk, Moscow Province, Russia

A quasisteady-state periodic structure established in a low-temperature, high-pressure, beam-driven discharge plasma in mixtures of hydrogen with inert gases is investigated experimentally and theoretically. The structure is observed through strong modulation of the luminescence intensity and density of the gas in the form of strata oriented perpendicular to the applied electric field. The physical cause of such stratification of a current-carrying plasma with a nonmonotonic field dependence of the positive-ion flux is attributed to a change in the ion species. © *1996 American Institute of Physics.* [S1063-7761(96)01010-4]

1. INTRODUCTION

The low-temperature gas-discharge plasma is a well-known example of a highly nonlinear self-organizing system. The diverse nonlinear structures observed under various conditions (filaments, moving and standing strata or layers, electrode hot spots, etc.) are usually explained by a theory based on a model that works with two diffusion-type equations as an essential element.[1,2] The driving force for the generation of inhomogeneous structures in this case is the nonlinearity of the source terms in these equations or the nonlinearity of the diffusion or thermal conduction transport coefficients. A detailed classification of the observed phenomena is discussed in Refs. 1 and 2, along with problems of the stability and kinetics of the stabilization of nonlinear structures for these conditions. Diffusion and thermal conduction transport processes become negligible within the characteristic scales for a discharge plasma in a gas at elevated pressure. Processes involving the drift of charged particles come to the fore in this case. Continuity of the total current and quasineutrality of the plasma give rise to effective convective fluxes whose velocity depends on the charged-particle density.[3] As in ordinary gas dynamics, this can lead to wave-breaking solutions or, in other words, to the onset of moving or stationary discontinuities in the charged-particle densities.[3] The dependence (which is more complicated than in gas dynamics) of the effective plasma transport velocity (which we call the ambipolar drift velocity) produces a greater diversity of possible phenomena: not only shocklike discontinuities, but also discontinuities at the wavefront in the form of a rarefaction wave. In reality, naturally, these discontinuities (abrupt changes or jumps) have a finite thickness, which is determined by higher-order transport processes (e.g., diffusion) or by the violation of quasineutrality. As in the theory of shock waves, these processes influence only the structure of the jump, which would naturally be called a drift jump.

In Ref. 4 the first experimental observation was described of a standing periodic luminous structure in a discharge in an $H_2(D_2)$:Ar mixture at a pressure of ≥ 1 atm, in which ionization was maintained by a beam of fast electrons with current density $J_b \sim 100$ μA/cm^2 and energy ≈ 120 keV. This structure was interpreted as a system of jumps caused by the special dependence of the ambipolar drift velocity of the plasma on the plasma density. The closest physical analog of the problem for time-independent strata with a similar mathematical structure is the phenomenon of shock waves in a mechanical system with a material particle of small mass moving under the influence of potential forces and friction.[5] The problem of the stabilization of such discontinuous periodic structures requires the development of a new mathematical apparatus in view of the singularity of the steady-state distributions. The attempt at direct mathematical modeling of a beam-driven discharge in an H_2:Ar mixture[6] has failed to show any progress (owing to the complexity of the computations) in physical times corresponding to the evolution of a structure of this kind. It is important to note that the kinetic model of a plasma in an H_2:Ar mixture[7,8] embodies not only plasma-chemical reactions (~ 40 processes), but also the vibrational kinetics of H_2 molecules. To adequately describe the processes of dissociative attachment of an electron to $H_2(v)$ molecules (v labels the vibrational levels) and the dissociation of an H^- ion in collisions with $H_2(v)$, it is necessary to include at least ten vibrational levels of H_2. Moreover, the evolution of the structures is complicated by the onset of domain instabilities and filaments.[6,8,9] Consequently, even one-dimensional modeling of a plasma in an H_2: Ar(He) mixture poses an exceedingly complex mathematical problem. Previously reported experimental data[4] have failed to provide an unambiguous interpretation of the observed structure as a steady-state periodic structure. The explanation proposed in Ref. 4 is therefore conjectural.

Similar luminous structures have also been observed in H_2:He mixtures.[10,11] No luminous strata were observed in an H_2:He mixture cooled down to 100 K.

Here we give the results of a detailed experimental study of the dynamics of the stratified structure of a beam-driven discharge in an H_2:Ar(He) mixture, along with the domain of parameters in which such structures exist. We derive a system of steady-state equations, which has a periodic solution under certain conditions. We analyze these conditions and clarify the mechanism by which they are established. We conclude that the interpretation proposed in Ref. 4 is valid.
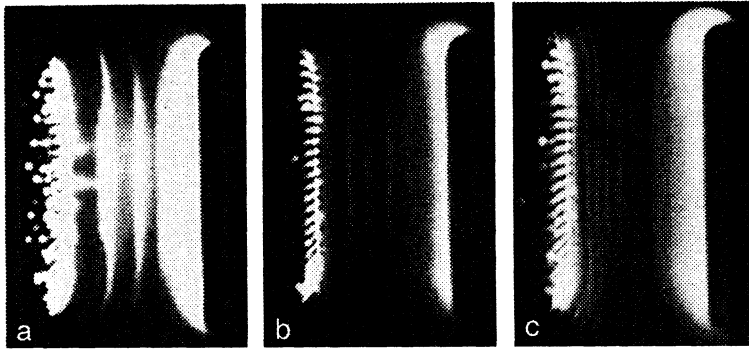
FIG. 1. Photographs of a discharge in a mixture of 10% H_2:Ar on an apparatus with 6×9 cm^2 electrodes. The interelectrode gap is 3 cm, the cathode is on the left, and $p = 1$ atm.

2. EXPERIMENTAL PROCEDURES

The existence of stationary strata in a beam-driven discharge in $H_2(D_2)$:Ar mixtures was first discovered on the device described in Ref. 4. The discharge was monitored by means of an electron beam with an energy of 120 keV and current density $J_b = 7-300$ μA/cm^2. The beam was injected through a grid electrode into the discharge gap with electrode dimensions and an interelectrode spacing ~ 1 cm. The experiments were performed in mixtures of $H_2(D_2)$:Ar gases at a pressure of 1-3 atm and room temperature. When an $H_2(D_2)$:He mixture was used, the discharge chamber could be cooled to liquid nitrogen temperature. This caused the stratification to disappear. The total emission of the discharge was recorded by a open-shuttered camera. The discharge was cut off until breakdown for a specified time interval by shutting off the applied electric field. In our work, simultaneously with the direct photography, on the same apparatus we recorded the discharge with a slow-motion device utilizing an FER-7 fast-framing/streak camera in conjunction with a PIM 103V image converter. We also recorded the emission from the electrode sheaths of the discharge by means of a system of slits, optical fibers, and photomultipliers.

In addition to these procedures, we used a Mach–Zehnder interferometer with a pulsed laser having a pulse duration of 18 ns. In one experiment we were able to obtain an eight-frame or 16-frame electron-optical photographic image of the discharge and a single interferogram at a specified time. To obtain a sequence of interferograms, the experiment had to be repeated as many times as necessary; this operation was facilitated by the excellent reproducibility of the result, as judged from oscillograms of the discharge current and the electron-optical photographs.

More detailed investigations of the evolution of the observed structures were performed on a larger apparatus utilizing an electron gun to inject a beam of cross section 6×9 cm^2 into the discharge volume. The electrode spacing was 2.5–3 cm. The emission of the discharge was investigated by means of a KADR framing camera equipped with a PV 001 image converter and a PMU optical intensifier. To further enhance the sensitivity, another KEDR amplifier was attached to the PMU. We used a slit of width 0.05 mm oriented along the discharge.

Most of the experiments were performed in mixtures of 10% H_2 with argon or helium. Given the low hydrogen con-

tent, the observed fringe pattern was complicated by the emergence of filaments and (or) domains in the interelectrode gap.[6,8,9]

Typical open-shutter photographs of the discharge (Fig. 1) obtained on the new large apparatus are similar to those obtained previously on the smaller apparatus.[4] Figure 2 shows interferograms of the discharge gap in the small chamber, and Fig. 3 shows the distribution of the gas density reconstructed from one of the interferograms. A comparison of these data with the results of fast-framing photography of the discharge shows luminous fringes accompanied by strong modulation of the gas density and, accordingly, its temperature. Estimates give a value of the gas temperature in the emission region ~ 700 K.

A vast quantity of information about the evolution of the disturbances has been obtained by means of the framing camera on the large apparatus. In the initial stage of discharge, depending on the conditions, we observe a complex pattern of evolution of the discharge and the formation of structures. In time periods $\sim 200-300$ μs a system of fringes parallel to the electrodes is visible in streak photographs, corresponding to stationary luminous strata. Typical streak photographs are shown in Fig. 4. At the onset of the discharge, a luminous stratum is formed at the anode and then vanishes, traversing up to a third of the interelectrode gap, depending on the strength of the field. In other experiments under similar conditions, photomultipliers have detected a burst of radiation in the vicinity of the anode. A domain moves from the cathode to the anode at a speed that increases with the strength of the field. In the anode sheath the plasma stratifies into a standing domain and a domain moving toward the cathode. As the field is increased, stratification sets in at an earlier time, and the oppositely moving domains begin to interact. In an even stronger field the plasma stratifies the front of the disturbance propagating from the cathode to the anode. A standing luminous structure has been observed in a 10% H_2:Ar mixture in the narrow interval of voltages $U_d = 4-6$ kV (interelectrode gap $d = 3$ cm) at beam currents $J_b \geqslant 14$ μA/cm^2. For beam currents higher than 160 μA/cm^2 instabilities (filaments) evolve within less than 200–300 μs, and luminous strata do not have time to form. It is interesting to note that the period of the structure at a fixed discharge voltage decreases roughly inversely with the square root of the beam current and increases directly with the discharge voltage (at a fixed beam
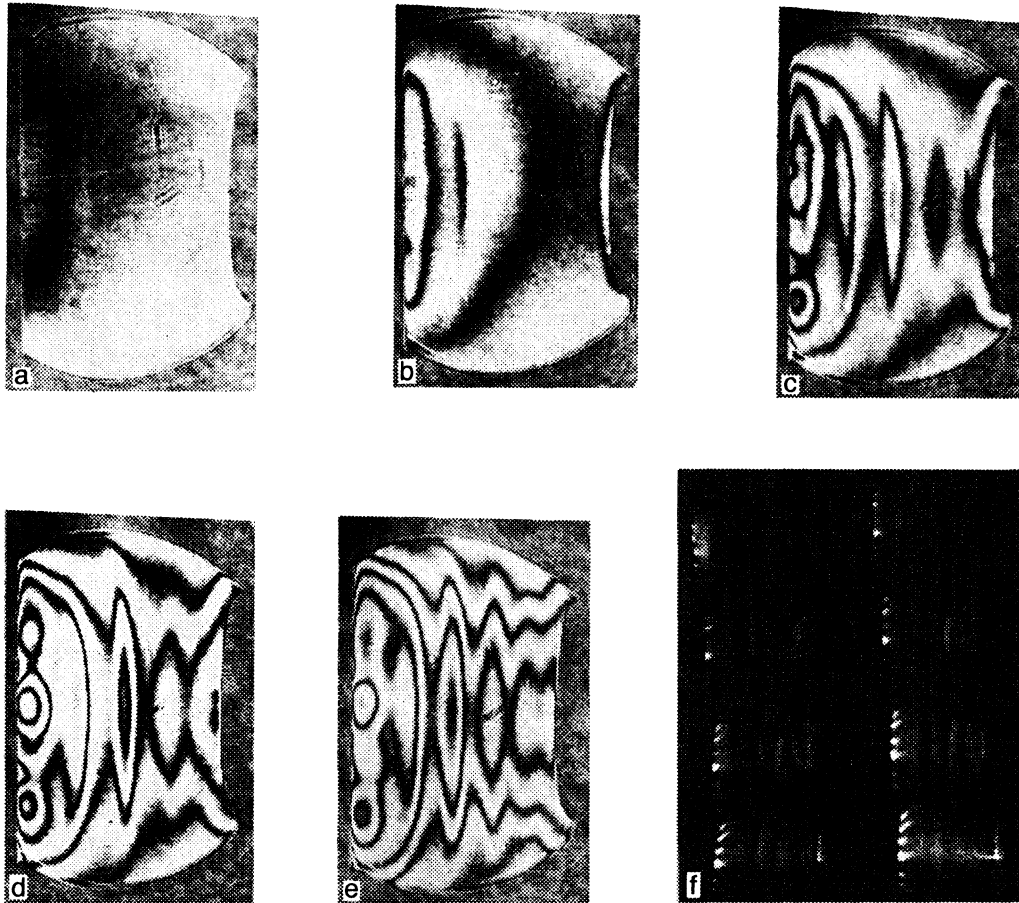
FIG. 2. Interferograms of a discharge in a mixture of 10% H_2:Ar at various times after the initiation of discharge: a) 20 μs; b) 80 μs; c) 180 μs; d) 220 μs; e) 280 μs; f) electron-optical photograph of the same discharge, frame exposure time and interval between frames 20 μs, frames sequenced from left to right and from top to bottom. The cathode is on the left. Discharge volume $1 \times 1 \times 1$ cm^3, $p = 1$ atm, $U_d = 2.2$ kV, $J = 0.5$ A/cm^2.

current). Similar results have been obtained in a discharge in a 10% $H_2(D_2)$:He mixture, where all the characteristic features of the H_2:Ar mixture were observed. In the He mixtures luminous strata have been observed in approximately the same range of parameters as in the Ar mixtures.

The reduced field E/N (E is the electric field strength, and N is the total density of particles) in a positive column
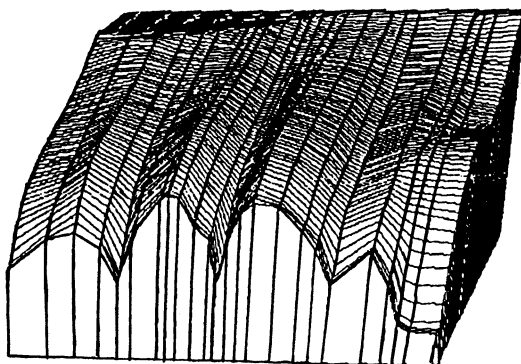

FIG. 3. Distribution of the gas density in half the discharge gap, reconstructed from the interferogram in Fig. 2d. The cathode is on the left, and the anode on the right.

determines the rates of processes involving electrons and depends on the voltage drop across the cathode sheath, which represents the sum of the normal cathode voltage (~ 150–200 V) and the voltage drop across the transition layer, and also on the fast-electron beam current J_b. For example, the extrapolation of the experimental current–voltage I–V characteristics of a discharge in H_2:He (Ref. 10) gives a cathode voltage of 400 V for $J_b = 200$ μA/cm^2 and 900 V for $J_b = 50$ μA/cm^2. When the beam current is lowered to 14 μA/cm^2, the cathode drop can increase to ~ 1800 V. Consequently, the reduced fields at which standing structures are observed to lie in the interval $(0.25$–$0.7) \cdot 10^{-16}$ V$\cdot$cm^2.

3. THEORETICAL MODEL

We now examine in closer detail the mechanism underlying the onset of standing structures in an H_2:Ar mixture. It follows from an analysis of the kinetic processes and numerical simulations[7,8] that the parameters and composition of a beam-driven discharge plasma remain virtually unchanged over the time (~ 30–50 μs) required to establish the vibrational distribution of H_2 molecules. Heating of the gas begins to exert its influence after 100 μs, causing the parameters to gradually change. When this happens, one negative
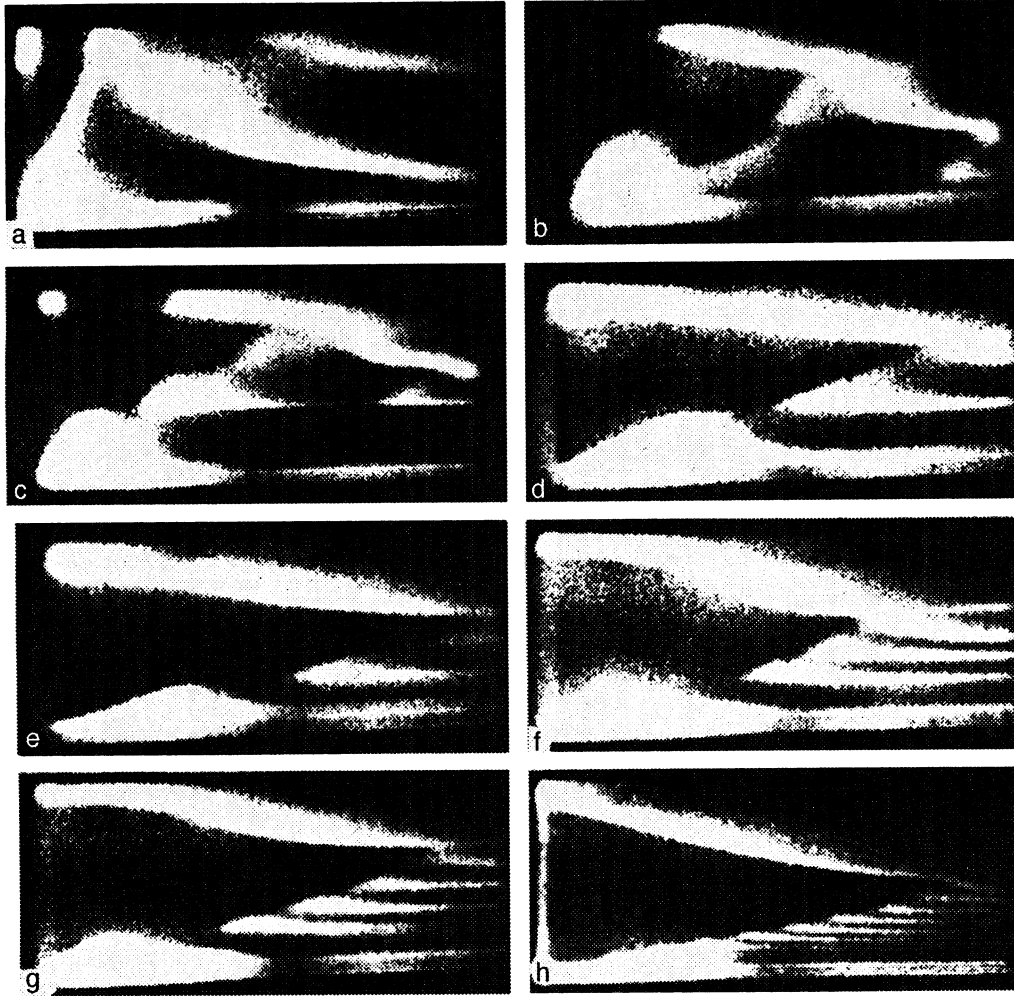
FIG. 4. Streak photographs of a discharge in a mixture of 10% H_2:Ar, $p=1$ atm, interelectrode gap 3 cm. The cathode is near the bottom. a) $J=236$ mA/cm^2, $U_d=7$ kV, streak time 200 μs; b) 80 mA/cm^2, 5 kV, 200 μs; c) 164 mA/cm^2, 5 kV, 200 μs; b) 267 mA/cm^2, 6 kV, 50 μs; e) 289 mA/cm^2, 6 kV, 50 μs; f) 200 mA/cm^2, 4 kV, 200 μs; g) 193 mA/cm^2, 4 kV, 200 μs; h) 311 mA/cm^2, 5 kV, 200 μs.

ion H^- ion and several species of positive ions H^+, Ar^+, Ar_2^+, ArH^+, and H_3^+ exist in the plasma. According to the calculations, the density of one of the ions dominates. We therefore consider a three-component plasma. The case of several positive ions can also be reduced to the case of one positive ion by introducing effective mobilities, diffusion coefficients, and recombination constants. The steady-state, one-dimensional charge transport equations for a three-component plasma are written in the form

$$\frac{d}{dx}\left(-\mu_e n_e E - D_e \frac{dn_e}{dx}\right) = S - \alpha n_e n_+ - \nu_a n_e + \nu_d n_- , \qquad (1)$$

$$\frac{d}{dx}\left(-\mu_- n_- E - D_- \frac{dn_-}{dx}\right) = \nu_a n_e - \nu_d n_- - \beta n_- n_+ , \qquad (2)$$

$$\frac{d}{dx}\left(\mu_+ n_+ E - D_+ \frac{dn_+}{dx}\right) = S - \alpha n_e n_+ - \beta n_- n_+ , \qquad (3)$$

where n_e, n_+, and n_- are the densities of electrons and positive and negative ions, respectively, μ_e, μ_+, μ_- and D_e, D_+, D_- are their mobilities and diffusion coefficients, S is the rate of ionization by a beam of fast electrons, ν_a and

ν_d are the frequencies of dissociative attachment of an electron and dissociation of a negative H^- ion in collision with atomic hydrogen and vibrationally excited $H_2(v)$ molecules,[7,8] and α and β are the electron–ion and ion–ion recombination rate constants.

The system of equations describing the self-consistent one-dimensional distribution of the plasma parameters is closed by the Poisson equation

$$\frac{dE}{dx} = 4\pi e(n_+ - n_- - n_e), \qquad (4)$$

where e is the electron charge.

In a beam-driven discharge the ion temperature differs little from the temperature of the gas, whereas electrons are heated considerably (with a characteristic energy of the order of 1 eV). Consequently, ion diffusion is negligible in comparison with the corresponding electrical drift, whereas for electrons diffusion transport processes can provide a substantial contribution. It is therefore advisable to replace Eq. (1) by continuity of the discharge current, a condition implied by

Eqs. (1)–(3). We write this condition in a form analogous to (1)–(4):

$$D_e \frac{dn_e}{dx} = \Gamma - E(\mu_e n_e + \mu_+ n_+ + \mu_- n_-), \qquad (5)$$

where $\Gamma = J/e$, J is the current density of the discharge, and ion diffusion is disregarded.[1] We rewrite Eqs. (2) and (3), again omitting ion-diffusion terms:

$$\frac{d}{dx}(-\mu_- n_- E) = \nu_a n_e - \nu_d n_- - \beta n_+ n_-, \qquad (6)$$

$$\frac{d}{dx}(\mu_+ n_+ E) = S - \alpha n_e n_+ - \beta n_+ n_-. \qquad (7)$$

The homogeneous state of the plasma at a given current density or electric field is determined by setting the right-hand sides of Eqs. (4)–(7) equal to zero. The distances over which the homogeneous state is established (relaxation lengths) are determined by comparing the left-hand side with the right-hand sides, and they are easily estimated.

1. Relaxation length for quasineutrality:

$$l_E = E/4\pi e n_+. \qquad (8)$$

2. Relaxation length for the electron drift current:

$$l_D = D_e/v_e, \qquad (9)$$

where v_e is the electron drift velocity.

3. In an H_2:Ar mixture (Refs. 7 and 8) dissociative electron attachment and negative-ion dissociation are much faster than the ion–ion and ion–electron recombination. The relaxation length for the balance of negative ions is therefore

$$l_- = \mu_- E/\nu_d. \qquad (10)$$

4. The relaxation length for the balance of positive ions is

$$l_+ = \mu_+ E n_+/S. \qquad (11)$$

Estimates based on the numerical model[7,8] and the parameters of the above experiments yield the following values: $l_E = 5 \cdot 10^{-4}$ cm ($J = 0.3$ A/cm^2, $J_b = 20$ μA/cm^2, $n_+ \cong 1 \cdot 10^{12}$ cm^{-3}); $l_D = 1.2 \cdot 10^{-3}$ cm ($p = 1$ atm, $E = 1$ kV/cm); $l_- = 1.7 \cdot 10^{-4}$ cm (the mobility of the H$^-$ ion in Ar is set equal to the mobility of an H$^+$ ion in Ar, $\mu_- = 6$ cm^2/V·s, by analogy with the mobilities of H$^+$ and H$^-$ ions in Kr: 8.9 cm^2/V·s and 9 cm^2/V·s, respectively); $l_+ = 0.12$ cm. Consequently, only the relaxation length for the balance of positive ions is of the order of the period of the experimentally observed strata and is much greater than all the other relaxation lengths. This justifies the use of Eq. (7) as a first approximation and the replacement of the remaining equations (4), (5), and (6) by the algebraic relations obtained when the right-hand sides are set equal to zero. A good candidate for the function sought as the solution of Eq. (7) is the

strength of the electric field E. To obtain relatively simple expressions, we observe the following inequalities, which are valid under the given experimental conditions: $\alpha n_e n_+ \ll \beta n_+ n_- \ll \nu_d n_-$ and $\mu_e n_e \gg \mu_+ n_+ + \mu_- n_-$. We note that their application is not fundamental to the ensuing discussion. These inequalities reduce Eq. (7) to the form

$$\frac{d\Phi(E)}{dx} = Q(E) = S - (\alpha + \beta\gamma)(1 + \gamma)\left(\frac{\Gamma}{\mu_e E}\right)^2, \qquad (12)$$

where $\gamma = \nu_a/\nu_d$, and $\Phi(E) = [1 + \gamma(E)]\Gamma\mu_+(E)/\mu_e(E)$. Here all the kinetic coefficients are functions, often complicated, of the field. The function $\Phi(E)$ is essentially an effective flux of the plasma, so that we can proceed in terms of a nonlinear ambipolar drift velocity.[3] Usually $\Phi(E)$ is a monotonic function of the field, and Eq. (12) has a homogeneous solution $E(x) \equiv E_0$. For a discharge driven by a fast-electron beam, E_0 is determined by the driver voltage U_d ($E_0 \cong (U_d - U_k)/d$, where U_k is the cathode drop, and d is the electrode spacing). A discharge current is established such that $Q(E_0) \equiv 0$.

It has been shown[4] by means of a complete kinetic model of the discharge processes that under certain conditions (beam current, discharge voltage, point in time, etc.) the ion flux $\Phi(E)$ becomes a nonmonotonic (sawtooth) function of the field. In this case we can construct a periodic solution $E(x)$ from pieces of the solution (12) with drift discontinuities of the field, at which the ion flux is preserved.

However, to justify the solution with drift discontinuities, we need to analyze it with allowance for the structure of the jump, i.e., retaining other derivatives. It follows from numerical estimates that the order of the left-hand sides of (4)–(6) relative to the right-hand sides is approximately identical. In this case the derivatives dn_e/dx and dn_-/dx can be expressed in terms of dE/dx on the basis of the relations obtained between n_e, n_-, and E by setting the right-hand sides of Eqs. (5) and (6) equal to zero: $n_- = \gamma n_e$; $v_e n_e = \Gamma$. Denoting $\hat{f} = d \ln f/d \ln E$, we obtain

$$\frac{dn_e}{dx} = -\Gamma \frac{\hat{v}_e}{Ev_e}\frac{dE}{dx}, \quad \frac{dn_-}{dx} = (\hat{\gamma} - \hat{v}_e)\frac{\gamma\Gamma}{Ev_e}\frac{dE}{dx}.$$

Next, expressing n_e from (5) and n_- from (6) and substituting them into the Poisson equation, we obtain the required equation with a small parameter for the derivative dE/dx:

$$\lambda \frac{dE}{dx} = E\left(1 - \frac{\Phi(E)}{\Gamma_+}\right), \qquad (13)$$

where

$$\lambda = l_E + \hat{v}_e l_D + \frac{\gamma}{1 + \gamma}(\hat{\gamma} - \hat{v}_e + \hat{v}_-)l_-,$$

$$\hat{v}_- = \frac{d \ln(\mu_- E)}{d \ln E}, \quad \Gamma_+ = n_+ \mu_+ E. \qquad (14)$$

We rewrite Eq. (12), using the function Γ_+ introduced above:
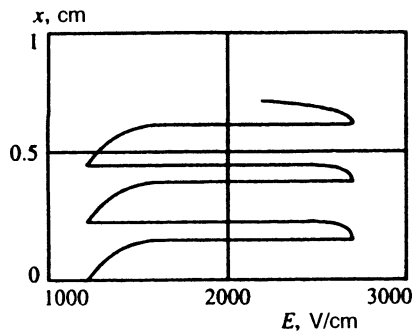
$$\frac{d\Gamma_+}{dx} = Q(E). \qquad (15)$$

FIG. 5. Example of a solution of the system (13) and (15) for $\lambda \ll L$.

We have thus obtained a system of equations (13), (15) that can be used under certain conditions (see below) to describe the experimentally observed periodic structures. Figure 5 shows an example of a solution of the system of equations (13), (15) in the case $\lambda \ll L$, where L is a characteristic length of the luminous stratum. It is obvious that the period of the structure Δ is determined by the form of the functions $\Phi(E)$ and $Q(E)$ and is equal to the integral with respect to the field E, evaluated around the contour $1-2-3-4$ in Fig. 6 (see below for the explanation of Fig. 6):

$$\Delta = \oint \frac{d\Phi(E)}{Q(E)}.$$

In order of magnitude this integral is equal to the relaxation length for the balance of positive ions l_+ (11). According to Refs. 7, 8, 10, and 11, the electron density in the plasma at room temperature is much higher than the negative ion density and is controlled by ion–ion recombination. This means that $n_+ \simeq n_e \sim \sqrt{S} \sim \sqrt{J_b}$. Consequently, the period of the structure increases with the voltage across the discharge and decreases with increasing beam current in accordance with the relation

$$\Delta \simeq l_+ \sim E/\sqrt{J_b},$$

which exhibits good agreement with the experimental results.

4. ANALYSIS OF CONDITIONS FOR THE ONSET OF PERIODIC STRUCTURES

As mentioned previously,[4] the system (13), (15) (with the variable x replaced by time) is well known in the theory of vibrations and describes discontinuous vibrations of a material point with friction.[5] An example of the solutions is given in the same paper.

Here we call attention to the fact that periodic solutions exist only for a certain behavior of the functions $\Phi(E)$ and $Q(E)$ and for the appropriate sign of λ in Eq. (13). For example, $\Phi(E)$ must be nonmonotonic, and $Q(E)$ must vanish in the region of nonmonotonicity. Assuming that $Q(E)$ is a monotonic function of the field in the vicinity of E_0 within the limits of interest, we infer that the integral curves of the system (13), (15) "ply a stable path" around the segments $1-2$ and $3-4$ shown in Fig. 6 and coincide in the direction of rapid variation of the field at the jump when either of two sets of conditions is satisfied:

$$\frac{d\Phi}{dE} < 0, \qquad \frac{dQ}{dE} < 0, \quad \lambda > 0 \quad \text{(Fig. 6a)}$$

or

$$\frac{d\Phi}{dE} > 0, \qquad \frac{dQ}{dE} > 0, \quad \lambda < 0 \quad \text{(Fig. 6b).} \tag{16}$$

In both cases the solution of the system (13), (15) is discontinuous (in the limit $\lambda/l_+ \to 0$) and periodic.

It is important to note that the calculations in Ref. 4 suggest the possibility of the first case (Fig. 6a) occurring at certain times in the evolution of the discharge in a H_2:Ar mixture. However, strata have also been observed experimentally in H_2:He mixtures.[10,11] Moreover, the homogeneous kinetic model used in Ref. 4 was only approximately valid for one-dimensional structures when transport processes were totally ignored. For these reasons we now analyze the more general situation in terms of the simplified kinetic model described here.

The possibility of satisfying either system of inequalities (16) is easier to estimate, beginning with the quantity λ, which characterizes the width of the expected jumps. We infer from the definition of λ (14) and the approximate values of the above-indicated plasma parameters that satisfaction of the condition $\lambda < 0$ is not very likely, because the sign of the largest term in (14) is determined by the sign of
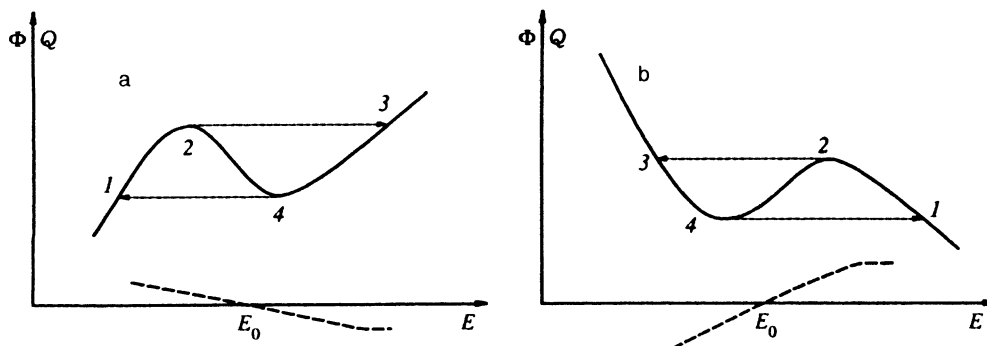

FIG. 6. Qualitative graphs of $\Phi(E)$ (solid curves) and $Q(E)$ (dashed lines) explaining the mechanisms of the onset of periodic structures for a) $d\Phi/dE < 0$; b) $d\Phi/dE > 0$.
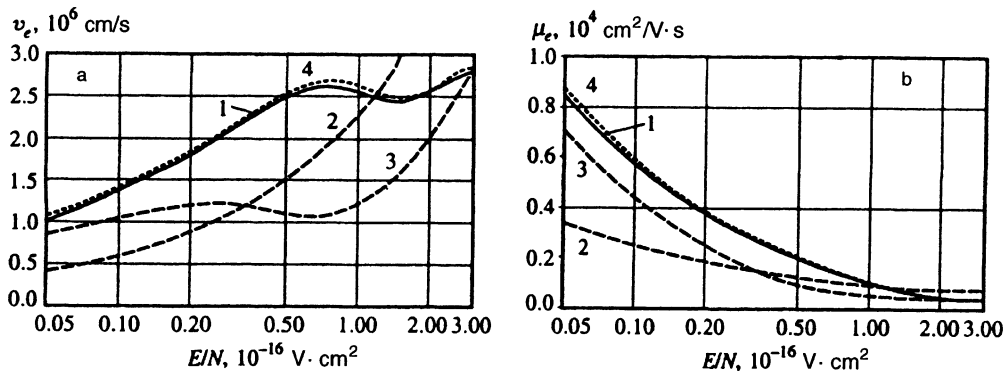
FIG. 7. Graphs of the drift velocity v_e (a) and mobility μ_e (b) of electrons vs E/N in H_2:Ar and H_2:He mixtures. *1)* 10% H_2:Ar; *2)* 10% H_2:He; *3)* 2% H_2:Ar; *4)* 10% H_2:Ar without vibrational excitation.

$\hat{v}_e$.[2] In this regard, the terms in (14) preserve their relationship over the entire range of beam currents, discharge voltages, pressures, and mixture constituencies investigated in the experiments. The condition $\lambda < 0$ requires satisfaction of the inequality $\hat{v}_e < 0$, i.e., the field dependence of the electron drift velocity would contain a descending segment. Such a segment does in fact occur in H_2:Ar mixtures, but in a range of electric fields other than those used in the experiments (Fig. 7). Check computations have shown that the vibrational excitation of H_2 does not appreciably alter the situation. Such a range is completely absent in H_2:He mixtures (Fig. 7). We note, in addition, that a rapid instability usually develops in the interval of electric fields corresponding to our $v_e(E)$ segment, causing domains to appear, which move with a velocity of order v_e (Refs. 6 and 8). In the discussion that follows, therefore, we can only analyze the first system of inequalities (16).

We wish to consider the factors responsible for the nonmonotonicity of the ambipolar flux $\Phi(E)$ (12); it can be attributed to the corresponding field dependence of the functions $\gamma(E)$, $\mu_+(E)$, and $\mu_e(E)$ (Fig. 8). In particular, $\gamma(E)$ can form a bell-shaped curve [$\gamma(E) \leq 1$], and $(\mu_+/\mu_e)(E)$ can be monotonic (Fig. 8a). The second scenario corresponds to the case where $[1 + \gamma(E)]$ is a weakly varying function in the interval where $\Phi(E)$ is nonmonotonic, and $(\mu_+/\mu_e)(E)$ is nonmonotonic. For an H_2:Ar mixture $\mu_e(E)$ is an explicitly decreasing function, and for an H_2:He mixture the electron mobility also decreases, but varies far less (Fig. 7b). Figure 8b qualitatively illustrates how the functions $\mu_e(E)$ and $\mu_+(E)$ should behave in order for the ratio μ_+/μ_e to exhibit nonmonotonic behavior.

4.1. Bell-shaped $\gamma(E)$ curve

Numerical modeling[7,8,10,11] shows that the bell shape of $\gamma(E)$ is caused by the field dependence of the rate of excitation of vibrational levels of H_2 and dissociative electron attachment to a vibrationally excited H_2 molecules. It is obvious that $\gamma(E)$ can influence the form of $\Phi(E)$ only when $\gamma(E)$ is not too small. Normally in calculations[7,8,10,11] the maximum value of γ is equal to 0.2–0.4 at room temperature and attains ~ 0.9 at 100 K. Figure 9 shows the $\gamma(E)$ curves for mixtures of 10% H_2 with Ar and He, calculated at a fixed gas temperature ($T = 300$ K and 100 K). In real situations the gas temperature varies with the field (as mentioned above, modulation of the gas density is observed in experiment), so that the $\gamma(E)$ curves in Fig. 9 give only a qualitative picture of the behavior of $\gamma(E)$. Obviously, the greater heating of the gas in stronger fields also tends to diminish γ. Consequently, the true $\gamma(E)$ curve has a sharper peak. For example, in calculations with heating of the gas taken into account[4] $\gamma(E)$ has a fairly narrow peak in order for the $\Phi(E)$ curve to be nonmonotonic. When heating of the gas is ignored, $\gamma(E)$ is a broader function of the field, and $\Phi(E)$ increases monotonically. We must also emphasize the lack of experimental information on the dissociation constants of H^- ions in collisions with $H_2(v)$, so that the true values of $\gamma(E)$ can differ from those obtained in the numerical calculations;[7,8,10,11] in particular, the variations of $[1 + \gamma(E)]$ may not be sufficient to produce the curve shown in Fig. 6a. To arrive at a final conclusion as to the prevalence of the first (Fig. 8a) or second (Fig. 8b) mechanism of the onset of a nonmonotonic $\Phi(E)$ curve, we analyze the com-
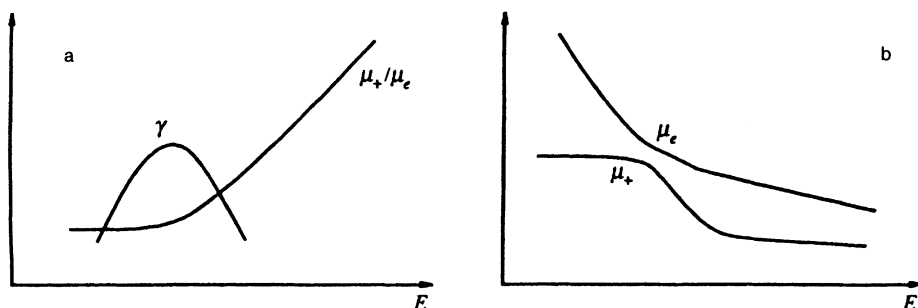

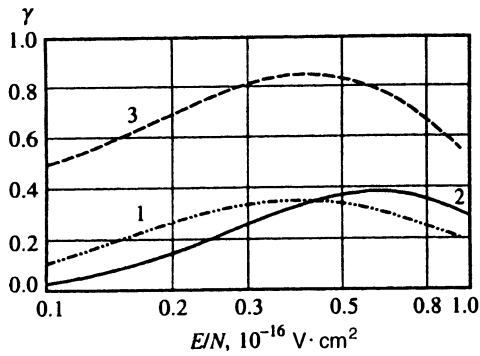FIG. 8. Qualitative dependence of various functions on field.

FIG. 9. Calculated graphs of $\gamma = \nu_a / \nu_d$ vs E/N in hydrogen–argon mixtures. *1)* 10% H_2:Ar, $T = 300$ K; *2)* 10% H_2:He, $T = 300$ K; *3)* 10% H_2:He, $T = 100$ K.

patibility of the postulated $\Phi(E)$ dependence with the condition that the source term in Eq. (15) decrease as the electric field increases. A $Q(E)$ curve (12) that decreases in the vicinity of $E = E_0$ can be obtained if the second term on the right-hand side increases with the field. An analysis of the kinetic processes[7,8,10,11] shows that the discharge current in H_2:Ar(He) mixtures under the stated conditions is controlled by ion–ion recombination ($\beta\gamma \gg \alpha$). Allowing for the fact that the electron drift velocity is an increasing function in this range of reduced fields (Fig. 7), we infer that the only way the second term can increase is for $\gamma(E)$ to increase with the field. Figure 10a shows graphs of $Q(E)$ at a fixed temperature. We note that in a mixture cooled to 100 K, owing to the weak relative variation of $\gamma(E)$ (Fig. 9), $Q(E)$ is a steeply increasing function, and standing structures cannot occur. The room-temperature $Q(E)$ curves (Fig. 10a) have a descending segment in the range of reduced fields $E/N \leq 0.25 \cdot 10^{-16}$ V·cm^2 for a mixture containing Ar and $E/N \leq 0.3 \cdot 10^{-16}$ V·cm^2 for mixtures containing He, i.e., for fields in which $\gamma(E)$ is an increasing function. But the range of nonmonotonicity of the flux $\Phi(E)$ due to the bell shape of $\gamma(E)$ is situated in the high field range, for which $\gamma(E)$ decreases as the field increases. Clearly, $Q(E)$ is an increasing function of the field in this range of the latter (Fig. 10a).

It is evident from the experiments that a periodic structure sets in at times of order 200–300 μs and is accompanied by strong modulation of the gas density. The influence of

heating of the gas on the occurrence of periodic structures is further evinced by the experimental observations of successive stratification during the cathode-to-anode transit of a domain that disrupts the initially homogeneous state of the plasma. We must therefore take into account the dependence of the rate of ionization by a fast-electron beam on the gas density. The thermal conductivity can be disregarded at such times (the characteristic thermal conduction time is ~ 0.7 μs for He and an order of magnitude greater for Ar). Consequently, under the given experimental conditions (constant gas pressure in the chamber) the ionization rate, which is proportional to the gas density, depends on the heating of the gas and, hence, on the field (constant current) as follows:

$$S = S_0 \exp\left(-\frac{\Delta\tau}{\tau_0}\frac{E}{E_0}\right), \tag{17}$$

where $\Delta\tau$ is the time elapsed from the passage of the domain, $\tau_0 = p_0 c_p / E_0 J$, p_0 is the gas pressure, $c_p = c_p / n_0 k$, c_p is the specific heat of the gas at constant pressure, k is the Boltzmann constant, and n_0 and S_0 are the particle density and the ionization rate at the time of passage of the domain. Estimates of τ_0 for the given experimental conditions ($p = 1$ atm, $T = 300$ K, $J = 0.5$ A/cm^2, $E_0 = 2.2$ kV/cm) give a value ≈ 280 μs, which is comparable with the time for periodic structures to form.

As the field is increased, the ionization rate decreases, which could cause the function $Q(E)$ to decrease in the range where $\Phi(E)$ is nonmonotonic. Calculations show, however, that the experimentally recorded heating in the given situation is not enough to establish the required dependence $Q(E)$, whereas in the case discussed below it produces a decreasing function $Q(E)$.

4.2. Nonmonotonicity of the function $\frac{\mu_+}{\mu_e}(E)$

If $[1 + \gamma(E)]$ varies only slightly, the mobility of positive ions in fields close to E_0 should drop steeply enough to ensure a nonmonotonic $\Phi(E)$ curve (Fig. 8b). This is possible only if there is a change in the species of positive ion. It should be borne in mind that the ion–ion recombination coefficient can also change in this case (see below). A lighter ion should dominate in a weak field, since a lighter ion generally has greater mobility.
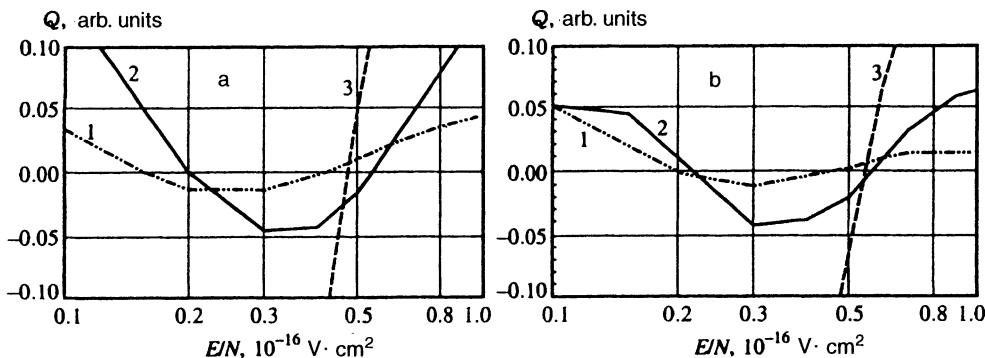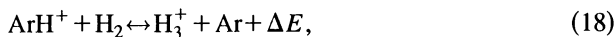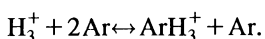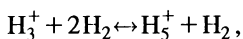

FIG. 10. Calculated graphs of the source term Q vs E/N without heating of the gas (a) and with heating of the gas taken into account (b). *1)* 10% H_2:Ar; *2)* 10% H_2:He; *3)* 10% H_2:He (100 K).

The forward and reverse reaction constants are used in Refs. 7 and 8:

$$ArH^+ + H_2 \leftrightarrow H_3^+ + Ar + \Delta E, \qquad (18)$$

whose ratio does not depend on the temperature of the gas. On the other hand, the energy deficit of this reaction is (Ref. 13, p. 422) $\Delta E = 0.53$ eV. Consequently, an increase in the gas temperature shifts the equilibrium of the reaction (18) toward an increase in the ArH^+ concentration. Such a change in the ion species from H_3^+ to ArH^+ has been observed in experiments to measure ion mobility in an H_2:Ar mixture.[14] In mixtures containing 1% or more H_2 an abrupt decrease is observed in the effective mobility, depending on the reduced field E/N, from 5.75 $cm^2/V \cdot s$ (the mobility of the H_3^+ ion under standard conditions) to 1.7 $cm^2/V \cdot s$ (the mobility of the ArH^+ ion). The effective mobility varies within a rather narrow interval of E/N. Mass spectrometer measurements of the ion current intensity show that in this interval of E/N the ion species changes from H_3^+ in weak fields to ArH^+ in strong fields. The values of E/N at which the mobility changes correspond to an average ion energy $\bar{\varepsilon} \approx 0.058$ eV or an effective temperature $T_{eff} = (2\bar{\varepsilon}/3k) \approx 670$ K $[\bar{\varepsilon} = (2/3) kT + (1/2)(M_i + M)W^2$, where M_i and M are the ion and neutral particle masses, and W is the ion drift velocity in the field], which is much smaller than the energy deficit of the reaction (18) (Ref. 13), but is consistent with estimates of the gas temperature in the emitting regions of the interferograms (see above). In the reaction (18) an H_3^+ ion is probably formed in vibrationally excited states and cannot make the transition to the ground state. Three-particle processes become important in the denser gas used in our experiments. In particular, the above-described ion–molecular reactions can be accompanied by the reactions[15]
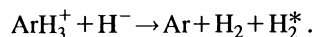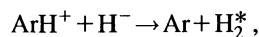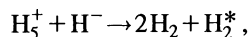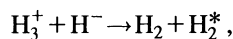
$$H_3^+ + 2H_2 \leftrightarrow H_5^+ + H_2,$$

$$H_3^+ + H_2 + Ar \leftrightarrow H_5^+ + Ar,$$

$$H_3^+ + 2Ar \leftrightarrow ArH_3^+ + Ar.$$

The binding energy in the $H_3^+ - H_2$ ion is equal to 0.35 eV (Ref. 15). We do not know the binding energy in the $H_3^+ - Ar$ ion. However, if this energy is lower than in the $H_3^+ - H_2$ ion, as is more than likely the case, the principal ion at low temperatures and in weak fields is H_5^+, but as the temperature increases this role is taken over by ArH_3^+, owing to the shift of the equilibrium of the reaction

$$ArH_3^+ + H_2 \leftrightarrow H_5^+ + Ar. \qquad (19)$$

The mobility of the H_5^+ ion is approximately equal to that of H_3^+ (Ref. 16). We do not know the mobility of the ArH_3^+ ion, but it should be lower than that of the H_5^+ ion and be close to the mobility of the ArH^+ ion. Consequently, our conclusions regarding the onset of nonmonotonicity of $\Phi(E)$ are also valid in the case of a denser gas by virtue of the change in the positive-ion species.

For stratification to take place, $Q(E)$ must also be a decreasing function in the range where $\Phi(E)$ is nonmonotonic [the first condition (16) and Fig. 6a]. At room temperature $Q(E)$ has a decreasing segment both in mixtures containing Ar and in mixtures containing He (Fig. 10a). However, the change in species of the principal positive ion is accompanied by changes in the ion–ion recombination constants of the processes[15,17]

$$H_3^+ + H^- \rightarrow H_2 + H_2^*,$$

$$H_5^+ + H^- \rightarrow 2H_2 + H_2^*,$$

$$ArH^+ + H^- \rightarrow Ar + H_2^*,$$

$$ArH_3^+ + H^- \rightarrow Ar + H_2 + H_2^*.$$

Although we do not know the constants of these processes, the recombination constant usually decreases as the reduced ion mass and the gas temperature increase:[15]

$$\beta = \frac{4.0 \cdot 10^{-7}}{\sqrt{mE_A}} \left(\frac{300}{T} \right)^{1/2}, \qquad (20)$$

where T is the gas temperature in kelvins, E_A is the energy for creation of an electron in a negative ion, and m is the reduced mass of the colliding ions in atomic mass units. In our case the ion recombination constant β depends weakly on the species of positive ion, since the reduced mass is determined mainly by the mass of the H^- ion. The decrease in β as an increase in the field raises the gas temperature $[T \sim 1/N \sim 1/S \sim \exp(\Delta \tau E/\tau_0 E_0)$, Eq. (17)] is not sufficient to eliminate the descending segment of the $Q(e)$ curve when the dependence of the ionization rate on the density (heating) of the gas is taken into account (Fig. 10b).

We emphasize that the ion–ion recombination constants determined from (20) have been used to plot $Q(E)$ of Eq. (12) in Fig. 10b. The heating of the gas has been specified on the basis of experimental estimates of the density modulation (Fig. 3) and corresponding to the parameter $\Delta \tau / \tau_0 \approx 1$ in (17).

Thus, the most probable mechanism for the onset of periodic strata is one for which the sawtooth profile of the ambipolar flux of positive ions is related to a change of species of the positive ion. A dearth of experimental information on the constants of the ion–molecular reactions involving complex ions and their mobilities and on the cross sections of the processes involving an electron prohibit us from indicating numerically precise boundaries for the parameters of the onset of a periodic structure. In particular, the theoretical model predicts that the interval of reduced fields for the existence of structure is from $0.1 \cdot 10^{-16}$ V $\cdot cm^2$ to $0.3 \cdot 10^{-16}$ V$\cdot cm^2$ (Fig. 10b), which is somewhat lower than the experimentally observed interval. On the other hand, the model explains experimentally observed trends such as the disappearance of structures when the gas is cooled, as well as the dependence of the period of the structure on the fast-electron beam current and the discharge voltage.

It has been remarked[18] that the steady-state solution of the system (13), (15) is unstable. Fluctuations of the distance between jumps in the $E(x)$ curve cause the solution to decrease until the structure "collapses." The experimental and theoretical results of the present study show that the onset of periodic structure is initiated by domain instabilities and is accompanied by perturbations of the density and temperature

of the gas, while the ion species changes as a result of heating of the gas. Under the investigated conditions, therefore, the system (13), (15) (with time terms included) is totally inadequate for analyzing the stability of the observed structures. It is necessary to invoke the gasdynamic equations.

This mechanism for the onset of luminous strata due to a change of species of positive ion is also valid for D_2:Ar, D_2:He, and H_2:He mixtures, where D_5^+ and H_5^+ ions predominate in weak fields, and ArD_3^+, HeD_3^+, and HeH_3^+ ions are prevalent in strong fields.

5. RESULTS AND CONCLUSIONS

A stationary periodic structure in a beam-driven discharge plasma in $H_2(D_2)$: Ar(He) mixtures at a pressure $\geqslant 1$ atm, consisting of luminous strata oriented perpendicular to the electric field, has been investigated experimentally and theoretically. Experimental investigations of the evolution of the observed structures have confirmed relaxation to a steady state. Interferometry of the discharge gap has shown that the appearance of luminous strata is accompanied by strong modulation of the density and, hence, the temperature of the gas, and their onset is initiated by a domain. When the mixtures are cooled to 100 K, stationary structures are not observed.

A steady-state, one-dimensional system of charge transport equations has been used in conjunction with the Poisson equation to describe the structure theoretically. An analysis of the results of zero-dimensional numerical modeling has enabled us to identify and estimate the values of the characteristic space scales in the given problem. The relaxation length for the balance of positive ions has been found to be two orders of magnitude greater than the relaxation length for the electron drift current and almost three orders greater than the relaxation length for quasineutrality of the plasma and the balance of negative ions. We have thus been able to reduce the basic system of equations to a system of two differential equations for the flux of positive ions and the field strength. In our case the flux of positive ions is an ambipolar plasma flux. The second equation for the derivative contains a small parameter, whose order of magnitude is determined by the smallness of all the other characteristic scale lengths in comparison with the relaxation length for the balance of positive ions. The first equation gives the so-called drift solution characterizing the period of the observed structure, and the second equation, with the small parameter, describes the jumps, i.e., abrupt changes of the field within a scale much smaller (in accordance with the value of the small parameter) than the period of the structure for an essentially invariant positive-ion flux. Such periodic solutions are known in wave theory as discontinuities.

Steady structures, i.e., periodic solutions, are possible in this system only under certain conditions: a nonmonotonic (sawtooth) field dependence of the ambipolar flux of positive ions, corresponding to the behavior of the source term in the first equation and the sign of the small parameter in the second equation. Here the positive-ion flux, the source term, and the small parameter are determined on the assumptions that the plasma is quasineutral, the discharge current is continu-

ous, and a stable negative-ion balance has been established. The positive-ion flux and the source term are rather complicated functions of the field, their form being determined by processes of dissociative attachment of an electron and dissociation of the H^- ion in collisions with vibrationally excited $H_2(v)$ molecules, electron–ion and ion–ion recombination, the electron and positive-ion mobilities, and the rate of ionization by the beam of fast electrons. The sign of the small parameter also depends on the relation between the relaxation lengths for the homogeneous solution and the negative-ion mobility. The complexity of the functional relations predetermines a variety of possible scenarios of the onset of periodic solutions.

A careful analysis of the conditions for the onset of structures using the results of zero-dimensional numerical modeling of a non-self-maintained discharge plasma in H_2:Ar(He) mixtures, along with calculations of the electron drift velocity and mobility in these mixtures has shown that a periodic solution occurs by virtue of a change in the species of positive ion, which imparts a nonmonotonic behavior to the ambipolar positive-ion flux. The required field dependence of the source term in the range of nonmonotonic behavior of the ambipolar flux is ensured only when, according to experiment, the influence of heating of the gas on the rate of ionization by the fast-electron beam is taken into account.

The conditions for the onset of structure impose strict limitations on the parameters of the plasma (such as the composition, the reduced field strength, and the temperature of the gas) and are established only at room temperature in mixtures containing $\approx 10\%$ H_2 within a narrow interval of reduced fields.

In summary, we have reported the first experimental and theoretical study of the stratification of a current-carrying plasma as a result of drift jumps analogous to gasdynamic shock waves.

---

[1])In the basic equations we have also emitted the term describing the electron flux induced by the inhomogeneity of the field (see, e.g., Ref. 12). The final equations are readily generalized to this case. However, calculations of the longitudinal and thermal diffusion coefficients by I. V. Kochetov in the range of fields where stratification is observed have shown that the thermal diffusion flux merely enhances longitudinal diffusion. Hence, it cannot lead to any new phenomena similar to thermocurrent instability.

[2])It is also possible for λ to change sign as a result of thermal diffusion flux. However, under the given conditions (see the preceding footnote) this does not happen.

---

[1] B. S. Kerner and V. V. Osipov, Usp. Fiz. Nauk **157**, 201 (1989) [Sov. Phys. Usp. **32**, 101 (1989)].

[2] B. S. Kerner and V. V. Osipov, Usp. Fiz. Nauk **160**(9), 1 (1990) [Sov. Phys. Usp. **33**, 679 (1990)].

[3] V. A. Rozhanskiĭ and L. D. Tsendin, *Collisional Transfer in a Partially Ionized Plasma* [in Russian], Énergoatomizdat, Moscow (1988).

[4] A. V. Dem'yanov, I. V. Kochetov, A. P. Napartovich *et al.*, Pis'ma Zh. Tekh. Fiz. **12**, 849 (1986) [Sov. Tech. Phys. Lett. **12**, 351 (1986)].

[5] N. V. Butenin, Yu. I. Neĭmark, and M. A. Fufaev, *Elements of the Theory of Nonlinear Oscillations* [in Russian], Nauka, Moscow (1976). [Prev. ed. transl. publ. by Blaisdell, New York, (1965)].

[6] A. V. Dem'yanov, I. V. Kochetov, A. P. Napartovich *et al.*, Fiz. Plazmy **15**, 487 (1989) [Sov. J. Plasma Phys. **15**, 284 (1989)].

[7] A. V. Dem'yanov, N. A. Dyatko, I. V. Kochetov *et al.*, Fiz. Plazmy **11**, 361 (1985) [Sov. J. Plasma Phys. **11**, 210 (1985)].

[8] A. V. Dem'yanov, N. A. Dyatko, I. V. Kochetov *et al.*, Fiz. Plazmy **12**, 623 (1986) [Sov. J. Plasma Phys. **12**, 359 (1986)].

[9] A. V. Dem'yanov, I. V. Kochetov, A. P. Napartovich *et al.*, Dokl. Akad. Nauk SSSR **306**, 1099 (1989) [Sov. Phys. Dokl. **34**, 540 (1989)].

[10] A. V. Dem'yanov, N. A. Dyatko, I. V. Kochetov *et al.*, Zh. Tekh. Fiz. **58**, 75 (1988) [Sov. Phys. Tech. Phys. **33**, 43 (1988)].

[11] A. V. Dem'yanov, I. V. Kochetov, A. F. Pal', and V. V. Pichugin, Zh. Tekh. Fiz. **60**(1) 204 (1990) [Sov. Phys. Tech. Phys. **35**, 124 (1990)].

[12] N. L. Aleksandrov, A. P. Napartovich, and A. N. Starostin, Fiz. Plazmy **6**, 1123 (1980) [Sov. J. Plasma Phys. **6**, 618 (1980)].

[13] I. S. Grigor'ev and E. Z. Meĭlikhov (eds.), *Physical Quantities* [in Russian], Énergoatomizdat, Moscow (1991), p. 422.

[14] K. V. McAfee Jr., D. Sipler, and D. Edelson, Phys. Rev. **160**, 130 (1967).

[15] B. M. Smirnov, *Complex Ions*, Nauka, Moscow (1983).

[16] B. M. Smirnov, *Ions and Excited Atoms in Plasma* [in Russian], Atomizdat, Moscow (1974).

[17] G. Bekefi (ed.), *Principles of Laser Plasmas*, Wiley, New York (1976).

[18] I. D. Kaganovich and L. D. Tsendin, in *Proceedings of the Conference on Low-Temperature Plasma Physics* [in Russian], Part 1, Petrozavodsk (1995), p. 116.

Translated by James S. Wood